



From Glymphatic System Dysfunction to Alzheimer's Disease: Mapping the Path of Neurodegeneration

Sha Li¹, Jinrui Zhang², Wenjing Wang², Shiling Zhou¹, Haoyu Wang¹, Mengfan Sun¹, Xiaoyao Lin¹, Jun Liu^{2*}

1- Chongqing Emergency Medical Center, Chongqing University Central Hospital, School of Medicine, Chongqing University, Chongqing 400044, China

2- Medical Imaging Department, Chongqing Emergency Medical Center, Chongqing University Central Hospital, #1 JianKang Road, YuZhong District, Chongqing 400014, China

*Corresponding Author: Jun Liu, liujluo@163.com, Medical Imaging Department, Chongqing Emergency Medical Center, Chongqing University Central Hospital, Chongqing, China;

Received: 15-01-2025

Accepted: 15-04-2025

Published: 02-12-2025

ABSTRACT

Background: The glymphatic system is intimately linked with the impaired clearance of abnormal proteins in Alzheimer's disease (AD); however, direct evidence demonstrating this mechanism in humans is still limited. The potential of the glymphatic system to predict AD pathology, neurodegeneration, clinical progression, and conversion to A β positivity, as well as its sequential relationship with core biomarkers at different stages of AD, warrants further investigation.

Aim: Explore the relationship between glymphatic activity and the pathological features and clinical progress of AD.

Materials and Methods: A retrospective analysis of participants from the ADNI who underwent amyloid PET, MRI, and neuropsychological assessments. The study included individuals with AD (79.12 \pm 8.66 years old; 17 males), mild cognitive impairment (MCI, 77.30 \pm 7.98 years old; 12 males), and cognitively normal (CN, 78.22 \pm 6.50 years old; 16 males) with a two-year follow-up. Whole-brain glymphatic activity measured by diffusion tensor imaging analysis along the perivascular space (DTI-ALPS).

Results: A faster decrease in the ALPS-index corresponds to a quicker A β deposition and a faster cognitive function decline ($p=0.01$). In the MCI-AD group, the accelerated turning point of the ALPS-index preceded A β deposition, while in the CN, MCI, and AD groups, it was later than A β deposition. The relationship between A β deposition and cognitive decline is fully mediated by the ALPS-index. A lower ALPS-index predicted higher A β burden and more severe cognitive decline ($p<0.001$), an increased risk of AD progression (HR = 2.5, 95%CI: 1.7, 3.7, $p<0.001$), and an increased risk of conversion to A β positivity (HR = 3.0, 95%CI: 1.6, 5.6, $p<0.001$).

Conclusion: Glymphatic dysfunction occurs prior to amyloid pathology and plays a pivotal role in A β deposition, heralding AD amyloid deposition, neurodegeneration, clinical progression, and conversion to A β positivity. The glymphatic system in the MCI stage exerts a protective effect on cognitive function in patients.

KEYWORDS

Glymphatic system; Alzheimer's disease; Mild cognitive impairment; DTI-ALPS; Cerebrospinal fluid biomarkers; Neurodegeneration

INTRODUCTION

The discovery of the glymphatic system and meningeal lymphatics has unveiled a novel pathway for the clearance of metabolic waste in the central nervous system. [1] Alzheimer's disease (AD) is pathologically characterized by the formation of amyloid- β plaques, primarily composed of amyloid- β peptide 42 (A β 42), and neurofibrillary tangles, predominantly consisting of Tau protein. Changes in cerebrospinal fluid (CSF) A β and Tau proteins are closely related to clinical symptoms of AD. [2, 3] The glymphatic system is intimately associated with the impaired

clearance of soluble A β [4] and Tau [5, 6] proteins in AD. Glymphatic system dysfunction is closely linked to the impaired clearance of soluble A β [4] and Tau [5, 6] proteins in AD. However, the relationship between glymphatic activity and AD biomarkers has been inadequately studied in humans. Mild cognitive impairment (MCI) is a high-risk prodromal phase of AD, with MCI subjects potentially progressing to AD and other neurodegenerative dementias, remaining stable, or even reverting to normal cognition. [7] According to the amyloid cascade hypothesis, abnormal A β deposition in the brain preced-

-es the decline in cognitive function and other clinical symptoms, potentially reaching a peak during the MCI stage. [8] Early A β and tau deposition are synergistically associated with cognitive decline. [9] Elucidating the changes in glymphatic activity and disease transition mechanisms from the MCI phase to the AD phase may pave the way for new methods to prevent or delay the onset of AD.

Diffusion tensor image analysis along the perivascular space (DTI-ALPS) technology is currently the most widely used non-invasive, real-time MRI technique for assessing glymphatic activity in humans. [10] Jack et al. [11] have shown that sequential changes in A β -tau neurodegeneration lead to cognitive decline, and glymphatic system dysfunction is the final common pathway for AD and other primary neurodegenerative diseases. [12] In-depth research on the dynamic changes and role of the glymphatic system in the clinical progression of AD, along with exploring the association between glymphatic activity and AD disease characteristics at different pathological and biological stages, may provide new insights for early diagnosis and treatment of AD.

We utilize the ALPS-index as a representation of glymphatic activity, in combination with amyloid- β PET, delve into the relationship between the ALPS-index and AD clinical and pathological features (cognitive scores, CSF, and neuroimaging biomarkers) at different biological and pathological stages of AD. We study the dynamic alterations of the ALPS-index with the standardized uptake value ratio (SUVR) from PET images and neurodegeneration in the clinical progression of AD. Regression models are established to explore the potential of glymphatic activity and core AD biomarkers to forecasting AD clinical progression and A β positivity conversion, as well as their impact on disease progression risk.

MATERIALS AND METHODS

Participants

This study is a combination of cross-sectional and longitudinal research, with data primarily sourced from the Alzheimer's Disease Neuroimaging Initiative (ADNI) database (<https://adni.loni.usc.edu/>). The ADNI study has received approval from the local Institutional Review Boards of all participating centers. For more detailed and up-to-date information on ADNI, please visit <https://www.adni-info.org>. All participants included in the study underwent neuropsychological assessments, 18 F-AV45 PET scans, and head MRI scans, with these examinations repeated after two years, capturing demographic and clinical information at two time points. The study involved 85 participants (170 examination data), including cognitively normal (CN=28) controls and individuals with cognitive impairment (CI=57), with the CI group comprising patients with MCI(N=24), MCI patients who converted to AD (N=16), and AD patients (AD=17). Neuropsychological assessments included Preclinical Alzheimer's Cognitive Composite (PACC), Mini-Mental State Examination (MMSE), Clinical Dementia Rating Sum of Boxes (CDR-SB), and Montreal Cognitive Assessment (MOCA), with PACC scores being associated with the detection of early cognitive decline in AD patients, [13, 14] where higher scores indicate more normal cognition. ApoE gene polymorphisms are associated with AD risk, [15] particularly the E4 subtype, [16] which is related to the early onset of AD. [17, 18] Decreased levels of A β 42 in CSF and increased tau protein are early markers of AD, [19, 20] and CSF samples from some ADNI participants have had these biomarker concentrations measured using specific methods.

Imaging Data Acquisition

In ADNI, T1-weighted imaging, fluid-attenuated inversion recovery imaging, and DTI data were acquired for each participant using 3T scanners. Details of the imaging protocol can be found in the open-source document (<https://adni.loni.usc.edu/methods/documents/mriprotocols/>). All ADNI participants provided eligible PET data, such as A β (18 F-AV45) PET data.

Image Analysis

This study conducted brain structural measurements based on quality-controlled T1-weighted neuroimaging data. The SPM12 toolbox was utilized to standardize the participants' 18F-AV45 PET and T1-weighted MRI images to the MNI space and co-register the PET images to the MRI images, ensuring consistency with the original MRI scans. Multiple brain regions were selected as regions of interest (ROIs) from the standardized images according to the AAL atlas. The average standardized uptake value for bilateral ROIs was calculated based on each patient's weight, and the average SUVR was computed using the cerebral gray matter as a reference region. The CAT12 toolbox was employed to quantify brain region volumes, yielding gray matter volume (GMV), white matter volume (WMV), and cerebrospinal fluid volume (CSFV), and the gray matter volume fraction (GMVF) was calculated by dividing the gray matter volume by the intracranial volume (ICV). To calculate the ALPS-index, DTI images required preprocessing, extraction of b0 values, skull stripping, and correction of distortions caused by eddy currents and subject motion before fitting the data to obtain fractional anisotropy (FA) maps and mean diffusivity (MD) maps. ImageJ software 1.53e (<http://imagej.nih.gov/ij>) was used to delineate ROIs on FA_RGB maps, measuring the diffusion coefficients in the x, y, and z directions in both projection and association areas, and calculating the average bilateral ALPS-index value. A higher ALPS-index indicates better glymphatic system function. Figure 1 demonstrates the flow of the image analysis.

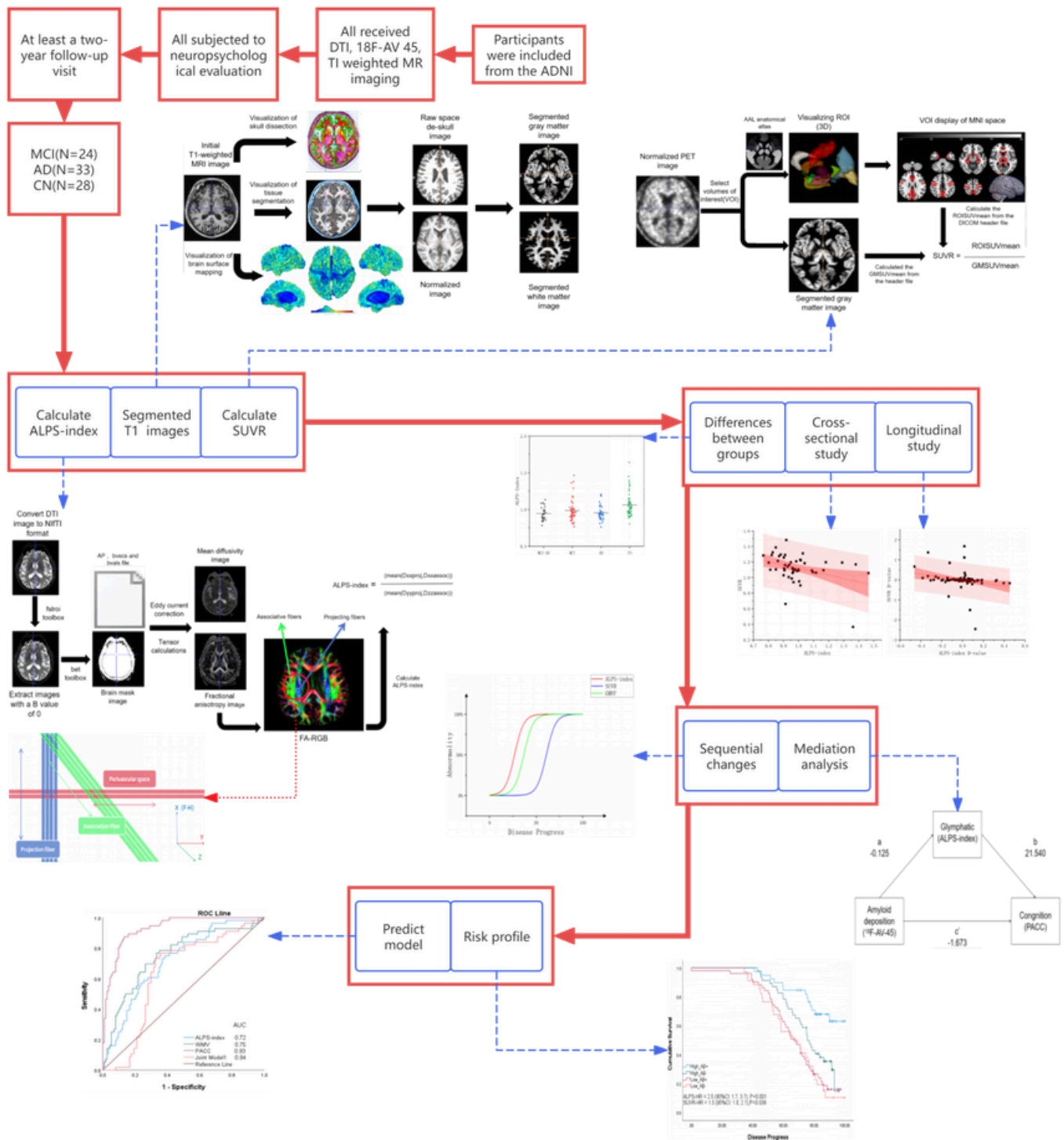
Statistical Analysis

This study utilized IBM SPSS Statistics27 software to conduct statistical analyses on the basic information and clinical scales of 85 subjects. Continuous variables were expressed as mean \pm standard deviation. Inter-group comparisons were performed using T-tests, Chi-square tests, and one-way ANOVA. Accounting for the effects of age, gender, years of education, and APOE4 alleles, linear regression was employed to analyze the cross-sectional and longitudinal relationships between the ALPS-index, AD biomarkers, neurodegenerative changes, and cognitive functions, with a significance level set at $p < 0.05$. Subjects were grouped based on A β positivity thresholds,[21] CSF A β 42 concentration thresholds,[22] and APOE4 genotypes to analyze the association between the ALPS-index and AD pathology and cognitive impairment. SUVR, ALPS-index, and GMVF data were normalized to 0~100%, PACC scores were used as a proxy for disease progression, and Sigmoid functions were utilized to model the trends of SUVR, ALPS-index, and GMVF changes. Using SPSS's PROCESS (Model 4) quantified the mediating variables to explore the mediating role of the ALPS-index between SUVR and cognitive impairment and GMVF,[23] and this was tested with the Bootstrap method,[24] confidence interval without zero as significant, the percentage of mediating effect (Pm) was calculated by dividing the indirect effect by the total effect to study the weight of the ALPS-index in the total effect across different groups.

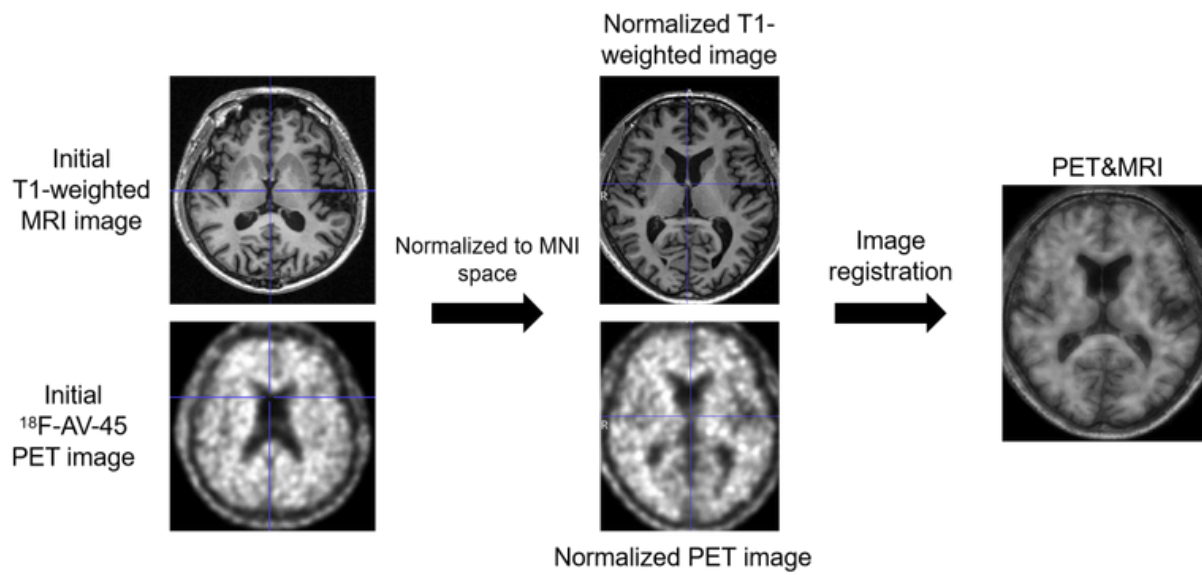
Furthermore, binary Logistic regression models were used to predict AD clinical progression and A β positivity conversion, with the Hosmer-Lemshow test assessing model fit. The ALPS-

index (< 0.997 and ≥ 0.997) and SUVR (< 1.11 and ≥ 1.11) were categorized as binary variables, and Kaplan-Meier curves and Cox regression models were used to investigate their impact on the risk of cognitive impairment and AD progression, with normalized PACC scores serving as the time variable in the Cox model.

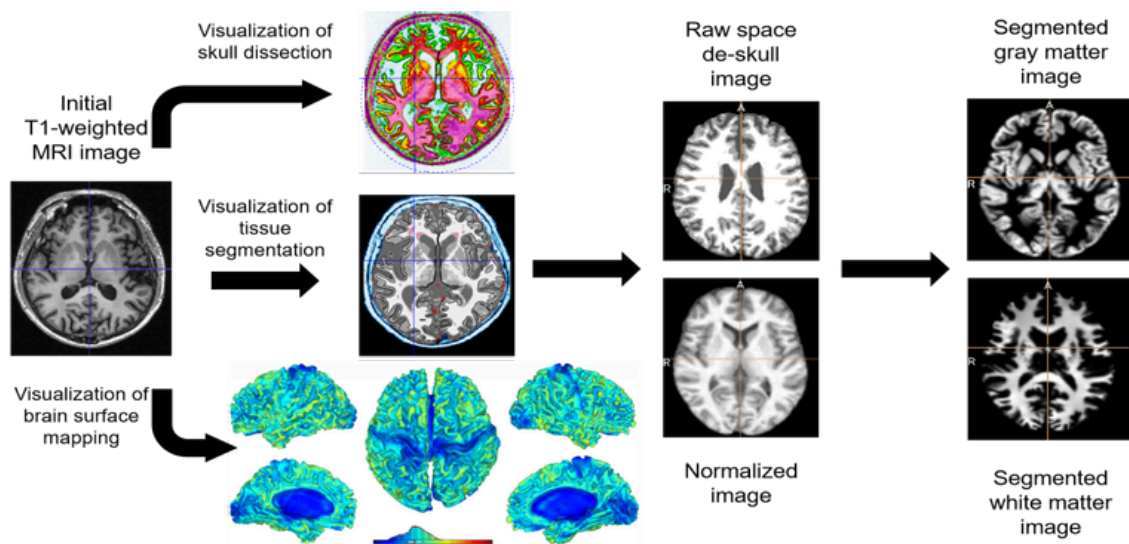
Figure1
(A) Overview of the study



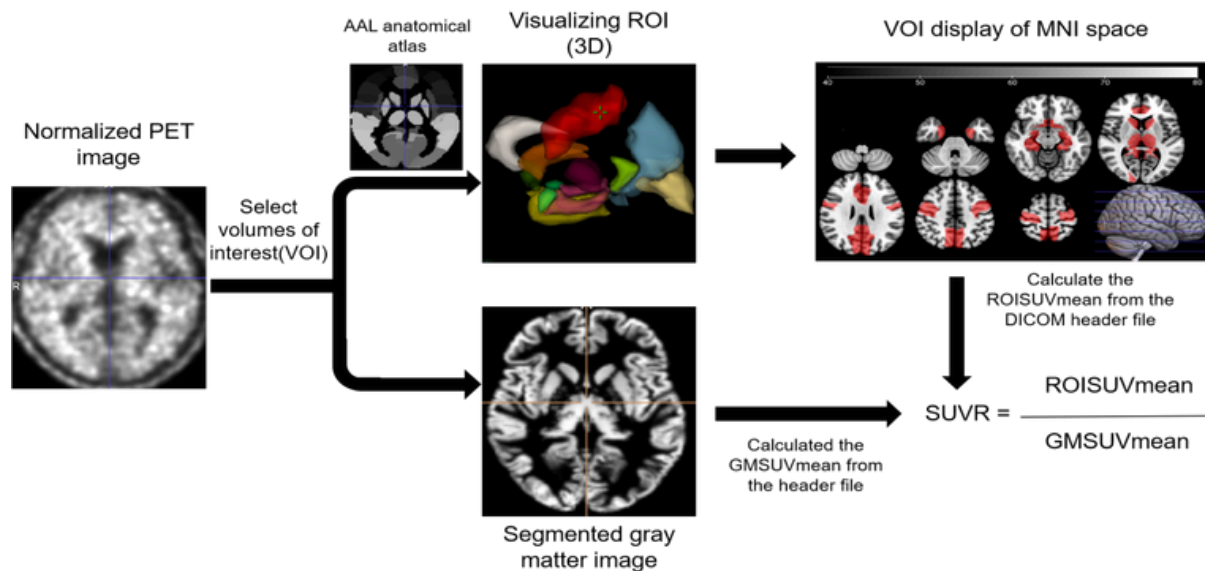
(B) T1-weighted image and PET image co-registration process



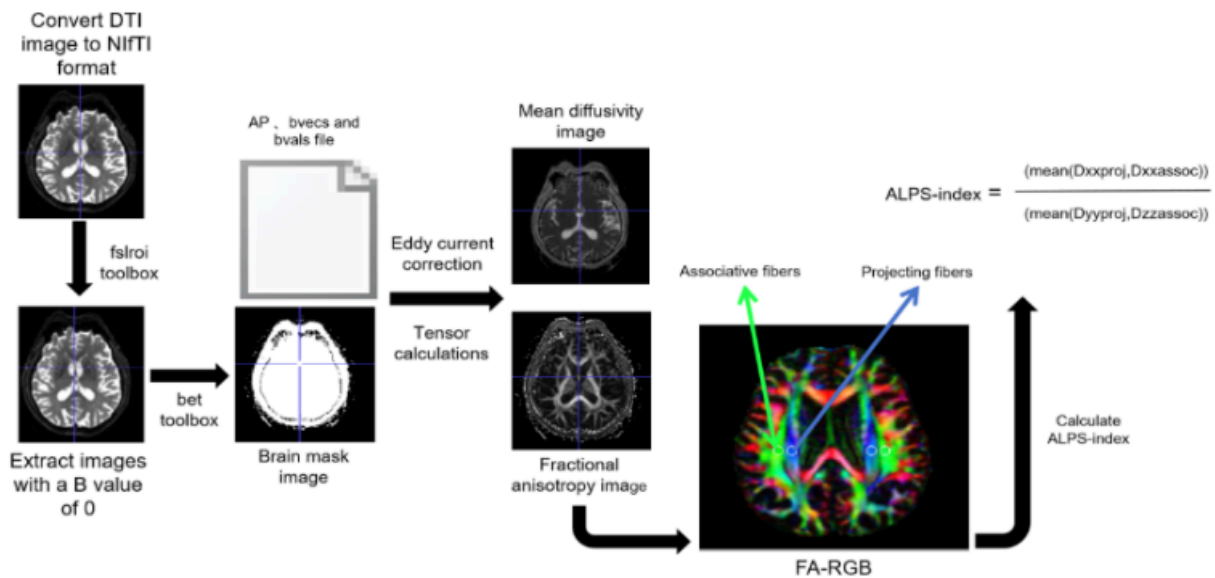
(C) T1-weighted image segmentation process of participants



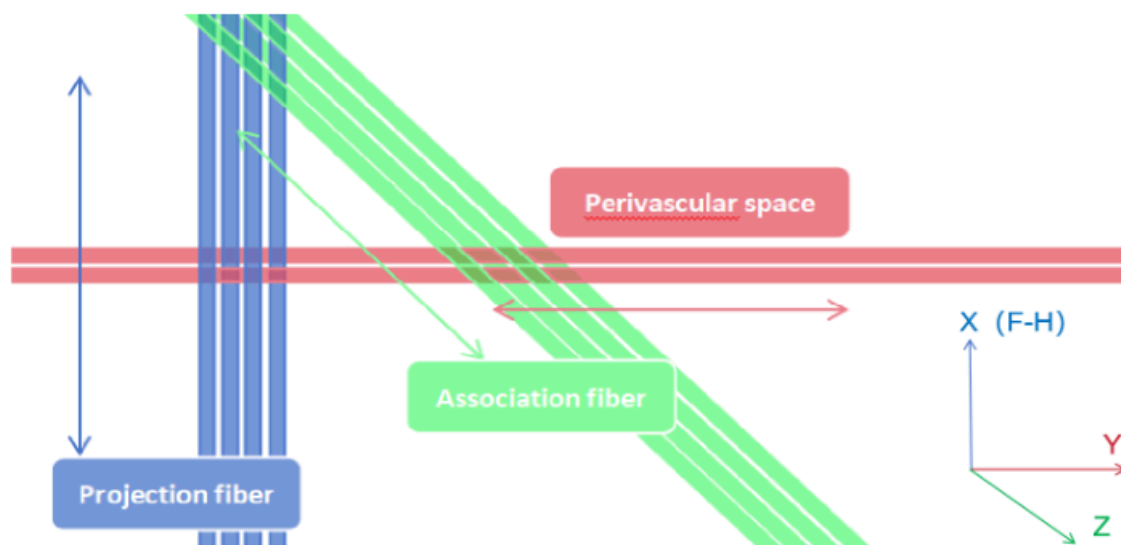
(D) SUVR quantification process



(E) ALPS-index calculation process



(F) Schematic representation of the relationship between PVS (red cylinders) orientation and fiber orientation in the left hemisphere of the brain



RESULTS

Demographic Data

Table 1 presents data from two examinations of the four groups including 57 CI patients (MCI-AD, MCI, AD) and 28 CN. Within the CI group, the CDR-SB scores two years later were significantly higher than those from two years prior ($p=0.03$, $p<0.01$). Between the CI and CN groups, all variables except for gender, age, ICV, GMV, GMVF, and SUVR showed significant differences ($p<0.01$). Table 2 shows data for the CSF A β + (<1098 pg/mL, N=26), CSF A β - (≥ 1098 pg/mL, N=9), A β +PET (≥ 1.11 , N=90), A β -PET (<1.11, N=80), APOE4+ (carrying the E4 gene, N=38), and APOE4- (without the E4 gene, N=47) groups. The differences among these groups are illustrated in Figure 2.

Table 1

TABLE 1. Demographic data and longitudinal clinical data

Characteristic	Total	CN	CI	MCI	MCI-AD	AD	P		
	(N=170)	(N=56)	(N=114)	(N=48)	(N=32)	(N=34)	ClvsC N	CNvsMCIvs MCI- ADvsAD	
Sex, male/female	45/40	46,007.00	29/28	46,003.00	45,877.00	45,878.00	0.45	0.96	
Education	15.95±2.55	17.46±2.04	15.21±2.44	15.13±2.51	15.81±2.14	14.76±2.66	<0.01	<0.01	
APOE4 genotype (positive:negative)	38/47	9/19	29/28	11/13	45,847.00	45,878.00	0.02	0.10	
Mean age, yr	77.30±7.80	77.22±6.52	77.38±8.37	76.32±7.97	75.63±8.90	80.54±7.83	0.89	0.04	
Mean ICV	1319.75±185.00	1306.77±171.65	1326.12±191.63	1334.72±179.05	1360.13±107.78	1281.98±256.78	0.52	0.32	
Mean volume of GM	538.06±113.16	531.38±121.99	541.34±108.97	544.14±99.11	550.55±71.77	528.73±146.88	0.59	0.82	
GM volume fraction	0.41±0.07	0.41±0.07	0.41±0.07	0.41±0.07	0.40±0.03	0.41±0.09	0.89	0.95	
Mean volume of WM	485.70±135.16	549.97±138.00	454.14±122.47	475.51±120.37	464.88±93.93	413.85±141.38	<0.01	<0.01	
Mean volume of CSF	295.98±127.58	225.42±104.30	330.64±123.97	315.08±132.39	344.69±110.06	339.40±125.15	<0.01	<0.01	
Mean ALPS indexes	1.00±0.14	1.06±0.16	0.97±0.12	0.97±0.15	0.95±0.09	0.95±0.11	<0.01	<0.01	
Mean cortical SUVR	1.17±0.33	1.22±0.39	1.15±0.29	1.13±0.18	1.12±0.34	1.23±0.35	0.25	0.28	
Mean FAQ score	5.76±7.93	0.84±3.29	8.18±8.42	2.46±3.81	9.03±7.72	15.44±7.97	<0.01	<0.01	
Mean MOCA score	22.26±4.23	25.71±2.10	20.56±3.97	22.98±3.24	19.44±3.23	18.21±3.72	<0.01	<0.01	
Mean MMSE score	26.45±3.67	29.05±1.20	25.17±3.80	27.44±2.17	25.56±2.33	21.59±4.11	<0.01	<0.01	
Mean CDR-SB score	2.19±2.77	0.17±0.44	3.17±2.90	1.23±1.00	3.02±2.30	6.07±2.86	<0.01	<0.01	
Mean PACC score	-13.83±15.88	0.62±6.52	-20.93±14.22	-10.51±8.91	-22.45±9.43	-34.19±12.42	<0.01	<0.01	
Longitudinal data							Total	CI	CN
	(N=85)	(N=26)	(N=57)	(N=24)	(N=16)	(N=17)			
Mean age, yr									
Before	76.35±7.77	76.22±6.50	76.41±8.38	75.34±8.01	74.73±9.03	79.51±7.90			
After	78.31±7.75	78.22±6.50	78.35±8.36	77.30±7.98	76.53±8.97	81.56±7.85	0.1	0.22	0.25
Mean ICV									
Before	1324.50±179.25	1307.83±170.16	1332.68±184.46	1337.63±176.66	1370.54±104.10	1290.07±246.31			
After	1315±191.53	1305.70±176.23	1319.57±199.96	1331.82±185.17	1349.72±113.75	1273.89±274.19	0.74	0.72	0.96
Mean volume of GM									
Before	541.13±111.07	522.85±120.84	550.11±105.91	544.03±86.74	561.77±57.98	547.72±158.41			
After	534.10±115.78	539.91±124.74	532.57±112.20	544.24±112.03	539.33±83.76	509.74±136.52	0.73	0.39	0.61

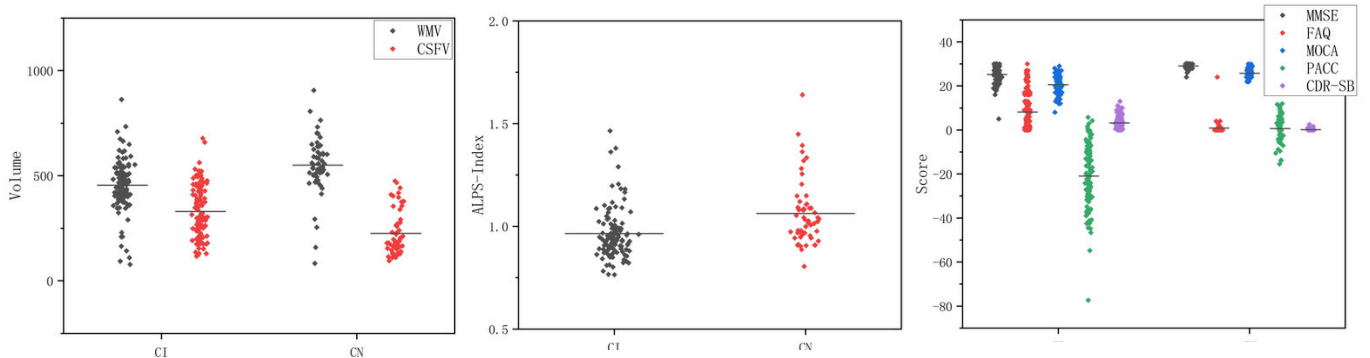
Mean volume of GM	Before	541.13±111.07	522.85±120.84	550.11±105.91	544.03±86.74	561.77±57.98	547.72±158.41	0.73	0.39	0.61
	After	534.10±115.78	539.91±124.74	532.57±112.20	544.24±112.03	539.33±83.76	509.74±136.52			
GM volume fraction	Before	0.41±0.06	0.40±0.07	0.41±0.06	0.41±0.05	0.41±0.03	0.42±0.09	0.86	0.56	0.36
	After	0.41±0.08	0.42±0.10	0.41±0.07	0.41±0.08	0.40±0.04	0.40±0.09			
Mean volume of WM	Before	499.61±118.81	562.74±107.93	468.60±112.18	494.23±96.22	484.85±81.52	417.12±142.98	0.18	0.21	0.49
	After	471.80±149.15	537.20±163.72	439.67±131.37	456.79±140.07	444.92±103.63	410.57±144.09			
Mean volume of CSF	Before	283.76±119.94	222.24±105.59	313.97±115.67	299.37±126.31	323.92±94.01	325.23±122.70	0.21	0.15	0.82
	After	308.21±134.39	228.60±104.82	347.31±130.64	330.79±139.09	365.47±123.60	353.57±129.70			
Mean ALPS indexes	Before	1.00±0.15	1.06±0.17	0.97±0.12	0.99±0.14	0.93±0.08	0.99±0.11	0.69	0.54	0.96
	After	0.99±0.14	1.06±0.14	0.96±0.12	0.99±0.16	0.96±0.09	0.92±0.09			
Mean cortical SUVR	Before	1.18±0.35	1.29±0.54	1.12±0.19	1.12±0.22	1.08±0.93	1.15±0.22	0.98	0.18	0.15
	After	1.17±0.30	1.14±0.08	1.19±0.36	1.13±0.12	1.16±0.48	1.31±0.43			
Mean FAQ score	Before	4.81±7.13	0.36±0.87	7.00±7.82	3.13±4.78	4.69±4.14	14.65±8.67	0.12	0.14	0.28
	After	6.71±8.59	1.32±4.55	9.35±8.90	1.79±2.43	13.38±8.11	16.24±7.39			
Mean MOCA score	Before	22.75±4.33	26.25±2.15	21.03±4.10	23.46±3.20	20.75±2.72	17.88±4.21	0.13	0.2	0.06
	After	21.76±4.09	25.18±1.93	20.09±3.82	22.50±3.27	18.13±3.24	18.53±3.26			
Mean MMSE score	Before	26.89±2.94	29.18±1.39	25.77±2.86	27.21±1.89	26.81±1.56	22.76±2.72	0.11	0.09	0.44
	After	26.00±4.25	28.93±0.98	24.56±4.50	27.67±2.44	24.31±2.33	20.41±4.94			
Mean PACC score	Before	-12.40±14.01	0.84±7.13	-18.90±11.80	-5.83±4.32	-9.27±3.75	-16.64±4.62	0.24	0.13	0.8
	After	-15.26±17.52	0.40±6.00	-22.95±16.13	-5.53±5.17	-14.29±4.80	-19.49±7.65			
Mean CDR-SB score	Before	1.72±2.32	0.20±0.55	2.46±2.48	1.06±0.91	1.38±0.85	5.47±2.45	0.03	<0.01	0.65
	After	2.65±3.11	0.14±0.30	3.89±3.12	1.40±1.08	4.66±2.11	6.68±3.18			

Table 1 Notes: Raw data were presented as mean (\pm standard deviation [SD]) or number in tables unless otherwise noted.

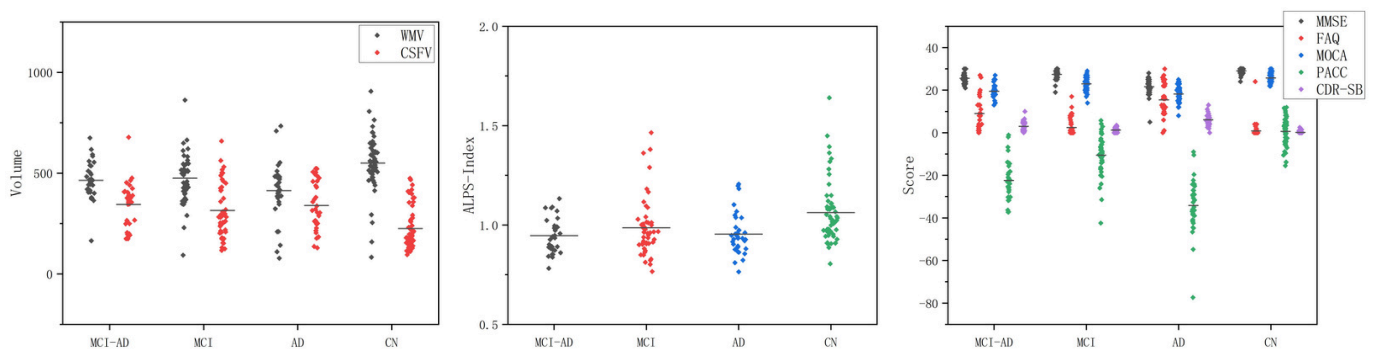
Abbreviations: ALPS, diffusion tensor image analysis along the perivascular space; APOE4, apolipoprotein E4; CI, cognitive impairment; CSF, cerebrospinal fluid; CN, cognitively normal; CDR-SB, Clinical Dementia Rating Sum of Boxes; FAQ, Functional Activities Questionnaire; GM, gray matter; ICV, intracranial volume; MOCA, Montreal Cognitive Assessment; MMSE, Mini-Mental State Examination; PACC, Preclinical Alzheimer's Cognitive Composite; SUVR, standardized uptake value ratio; WM, white matter.

Figure 2

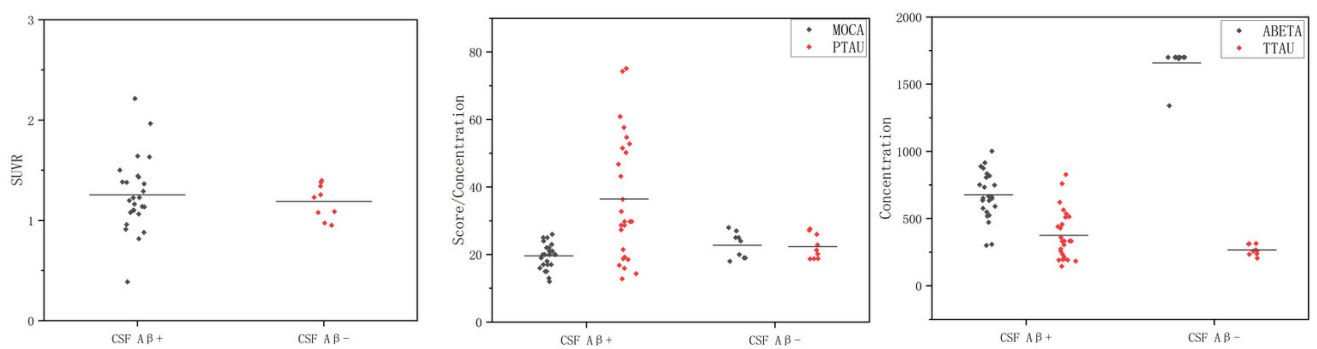
(A) Group differences in groups CI and CN



(B) Group differences in groups AD, MCI-AD, MCI and CN



(C) Differences between the two groups



(D) Differences between the two groups

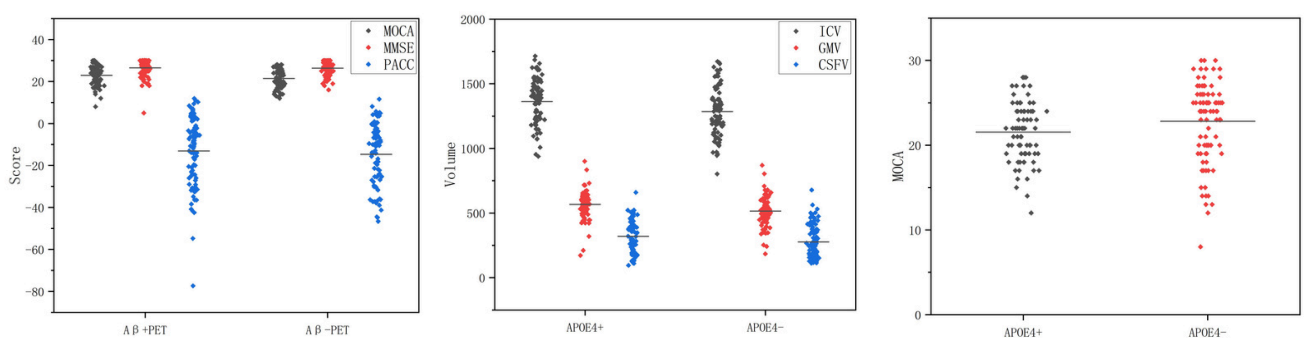


TABLE 2. Demographic data and clinical data from different groups

Characteristic	CSF A β +	CSF A β -	A β + PET	A β - PET	APOE4+	APOE4-	P		
	(N=26)	(N=9)	(N=90)	(N=80)	(N=38)	(N=47)	CSFA β +/-	A β PE T+/-	APOE 4+/-
Sex, male/female	12/14	6/3.	48/42	42/38	44/32	46/48	0.91	0.31	0.25
Education	15.27 \pm 2.59	15.56 \pm 2.30	16.18 \pm 2.42	15.70 \pm 2.67	15.37 \pm 2.54	16.43 \pm 2.45	0.23	0.76	0.07
APOE4 genotype (positive:negative)	10/16	6/3.	61/29	33/47			<0.01	0.79	
Mean age, yr	76.16 \pm 6.36	79.5 \pm 9.27	76.06 \pm 6.59	78.76 \pm 8.80	76.21 \pm 8.51	78.24 \pm 7.10	0.03	0.34	0.1
Mean ICV	1373.33 \pm 212.20	1345.20 \pm 158.6 0	1300.70 \pm 173. 65	1341.18 \pm 195.8 7	1363.05 \pm 179. 72	1284.73 \pm 182. 69	0.16	0.68	<0.01
Mean volume of GM	562.42 \pm 70.89	604.49 \pm 125.87	526.69 \pm 111.52	550.85 \pm 114.3 1	566.84 \pm 112.5 7	514.79 \pm 108.7 4	0.17	0.36	<0.01
GM volume fraction	0.41 \pm 0.05	0.45 \pm 0.07	0.41 \pm 0.07	0.41 \pm 0.08	0.42 \pm 0.08	0.40 \pm 0.07	0.52	0.21	0.15
Mean volume of WM	428.44 \pm 108.99	456.83 \pm 140.2 0	492.07 \pm 128.88	478.54 \pm 142.37	475.94 \pm 142.47	493.60 \pm 129.1 8	0.52	0.59	0.4
Mean volume of CSF	382.47 \pm 100.09	283.88 \pm 127.71	281.93 \pm 131.36	311.79 \pm 122.08	320.28 \pm 125.9 7	276.34 \pm 126.1 3	0.13	0.06	0.03
Mean ALPS indexes	0.93 \pm 0.11	1.00 \pm 0.14	0.98 \pm 0.14	1.02 \pm 0.14	1.00 \pm 0.14	1.00 \pm 0.14	0.07	0.21	0.99
Mean cortical SUVR	1.33 \pm 0.64	1.13 \pm 0.10	1.31 \pm 0.39	1.03 \pm 0.10	1.15 \pm 0.38	1.19 \pm 0.28	<0.01	0.13	0.4
Mean FAQ score	8.23 \pm 7.81	3.56 \pm 8.52	5.03 \pm 7.59	6.58 \pm 8.27	6.79 \pm 9.42	4.93 \pm 6.41	0.21	0.17	0.14
Mean MOCA score	19.62 \pm 3.63	22.78 \pm 3.80	23.00 \pm 4.16	21.43 \pm 4.18	21.54 \pm 3.51	22.84 \pm 4.67	0.02	0.04	0.04
Mean PACC score	-22.88 \pm 13.29	-9.83 \pm 7.78	-13.10 \pm 16.70	-14.65 \pm 14.96	-15.36 \pm 13.16	-12.60 \pm 17.75	0.52	<0.01	0.25
Mean MMSE score	24.88 \pm 3.04	27.89 \pm 1.96	26.54 \pm 3.95	26.34 \pm 3.36	26.41 \pm 2.88	26.48 \pm 4.22	0.71	<0.01	0.9
Mean CDR-SB score	2.93846 \pm 2.22	1.50 \pm 2.50	2.16 \pm 2.99	2.21 \pm 2.51	2.46 \pm 2.82	1.96 \pm 2.72	0.9	0.16	0.25
A β concentration, pg/mL	676.37 \pm 173.06	1658.78 \pm 119.6 0					<0.01		
TTAU concentration,pg/ mL	374.43 \pm 182.29	266.56 \pm 38.88					<0.01		
PTAU concentration,pg/ mL	36.45 \pm 18.44	22.37 \pm 3.69					<0.01		

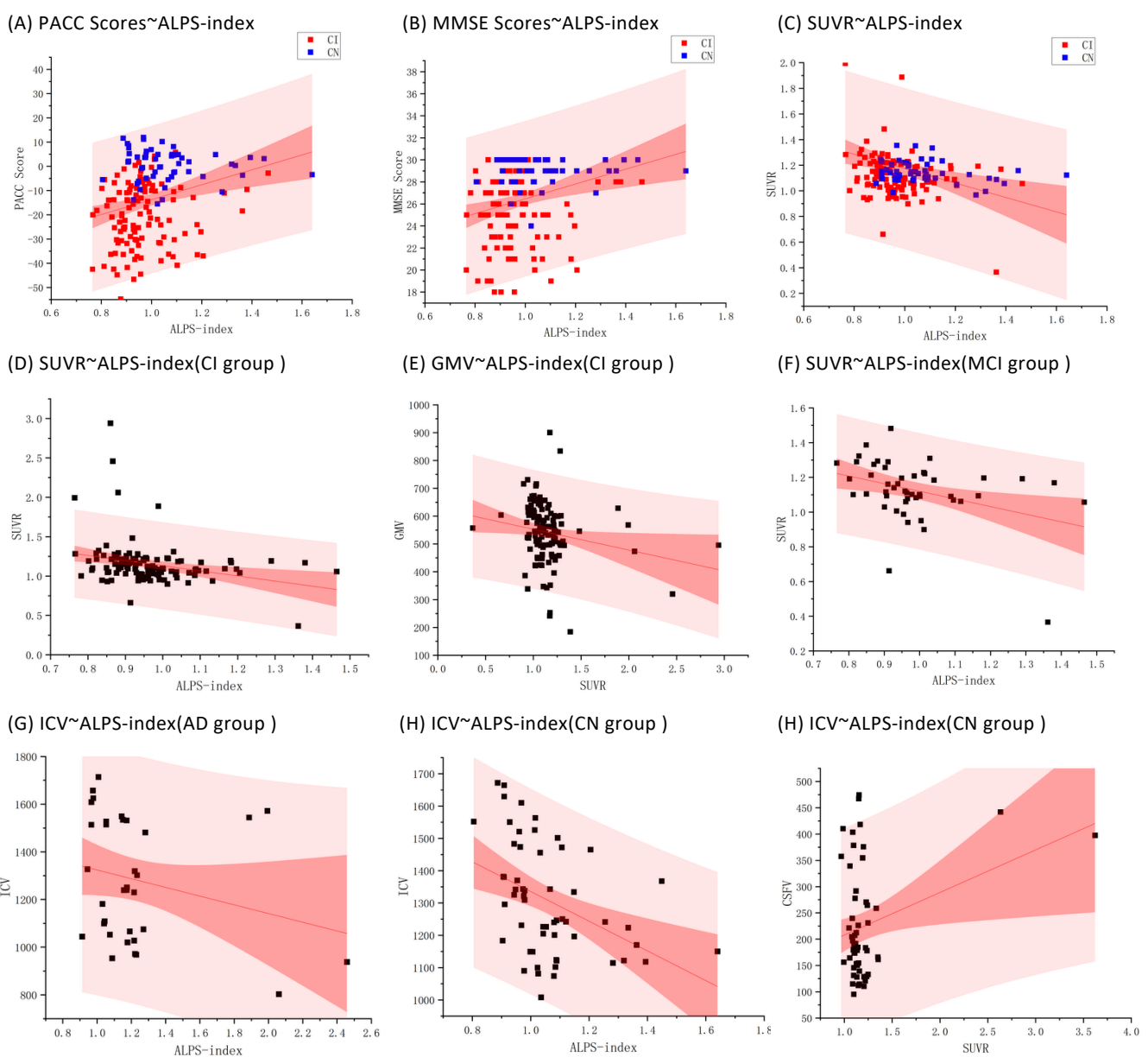
Table 2 Notes: Raw data were presented as mean (\pm standard deviation [SD]) or number in tables unless otherwise noted. Abbreviations: ALPS, diffusion tensor image analysis along the perivascular space; APOE4+, apolipoprotein E4 positive; APOE4-, apolipoprotein E4 negative; A β , amyloid beta; CDR-SB, Clinical Dementia Rating Sum of Boxes; CSF A β +,

cerebrospinal fluid A β positive; CSF A β -, Cerebrospinal fluid A β negative; CI, cognitive impairment; CSF, cerebrospinal fluid; CN, Cognitively normal; FAQ, Functional Activities Questionnaire; GM, gray matter; ICV, intracranial volume; MOCA, Montreal Cognitive Assessment; MMSE, Mini-Mental State Examination; PACC, Preclinical Alzheimer's Cognitive Composite; PTAU, phosphorylated tau protein; SUVR, standardized uptake value ratio; TTAU, total tau protein; WM, white matter.

ALPS-index associated with amyloid deposition and cognition at different pathological and biological stages of AD

Controlling for age, sex, years of education, and APOE4 genotype, the ALPS-index showed significantly positive correlations with PACC scores ($R^2=0.07$, $p<0.001$, Figure 3A), MMSE scores ($R^2=0.07$, $p<0.001$, Figure 3B), and MOCA scores ($p=0.002$), and significantly negative correlations with SUVR ($R^2=0.06$, $p=0.001$, Figure 3C), CDRSB scores, ICV, CSFV, and FAQ scores ($p<0.001$, $p=0.005$, $p=0.003$, $p=0.03$). In the CI group, the ALPS-index showed significantly negative correlation with SUVR ($R^2=0.08$, $p=0.003$, Figure 3D), and SUVR showed significantly negative correlation with GMV ($R^2=0.04$, $p=0.04$, Figure 3E). In the MCI group, the ALPS-index showed significantly negative correlation with SUVR ($R^2=0.14$, $p=0.006$, Figure 3F). In the AD group, SUVR and ICV showed significantly negative correlation ($R^2=0.06$, $p=0.04$, Figure 3G). In the CN group, the ALPS-index showed significantly negative correlations with ICV ($R^2=0.18$, $p=0.03$, Figure 3H) and CSFV ($p=0.03$), and significantly positive correlations with SUVR, CSFV ($R^2=0.09$, $p=0.04$, Figure 3I), and MOCA scores ($p=0.04$, $p=0.05$). The ALPS-index showed significant correlations with SUVR across all ROIs in patients ($p<0.05$).

Figure 3



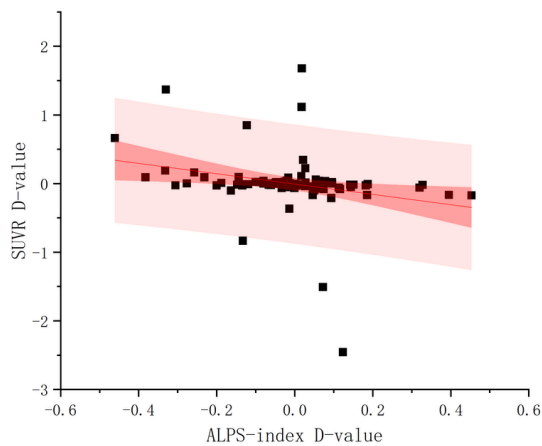
Longitudinal relationship of ALPS-index, SUVR in 18 F-AV45 PET images, and neurodegeneration

Controlling for sex, age, years of education, and APOE4 genotype, a faster decline in the ALPS-index rate was significantly associated with a faster increase in A β load ($R^2=0.07$, $p=0.01$, Figure 4A). A faster increase in A β load was significantly associated with a faster decrease in ICV ($R^2=0.01$, $p=0.04$, Figure 4B). The rate of change in WMV was significantly associated

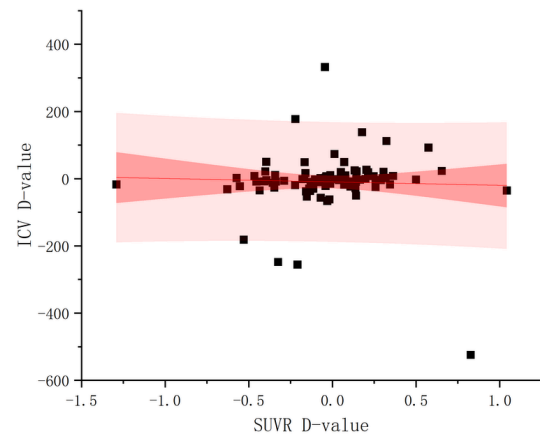
with the rate of change in GMV ($R^2=0.5$, $p<0.01$, Figure 4C) and the rate of change in cerebrospinal fluid volume (CSFV) ($R^2=0.16$, $p<0.01$, Figure 4D). Patients with GMV at the last examination less than at the previous examination were classified as GM atrophy patients (GMA, $N=56$), and others as non-GM atrophy patients ($N=29$). There were significant differences in the longitudinal changes of GMV, WMV, and GMVF between the two groups ($p<0.001$). In GMA patients, a faster decrease in GMVF rate was significantly associated with a faster decline in MMSE scores ($R^2=0.03$, $p=0.02$, Figure 4E), and a faster decline in the ALPS-index rate was associated with a faster increase in A β load ($R^2=0.08$, $p=0.03$, Figure 4F). The number of APOE4-positive patients differed significantly between the two groups ($p<0.001$), and patients carrying APOE4 had larger GMV than those not carrying APOE4, with a greater propensity for atrophy.

Figure4

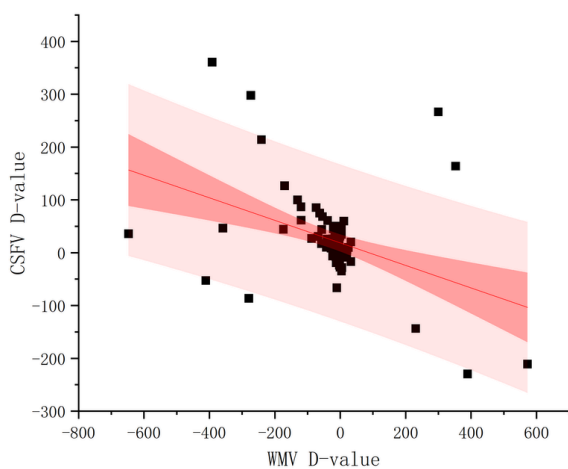
(A) 18 F-AV45 SUVR D-value ~ALPS-index D-value



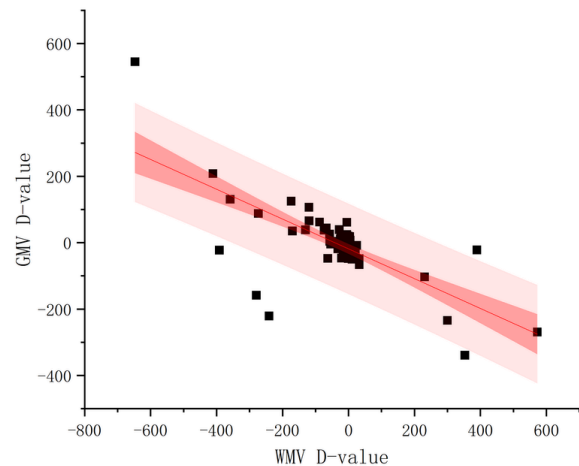
(B) ICV D-value ~SUVR D-value



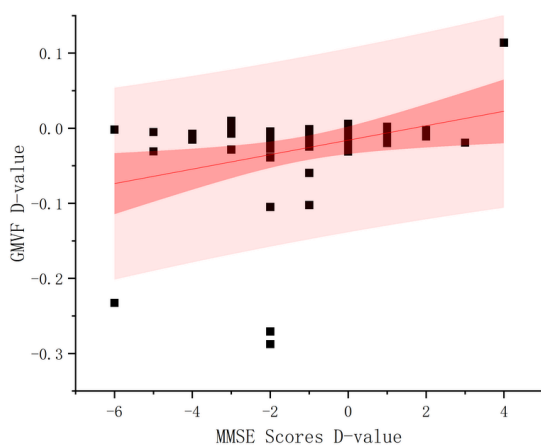
(C) CSFV D-value ~WMV D-value



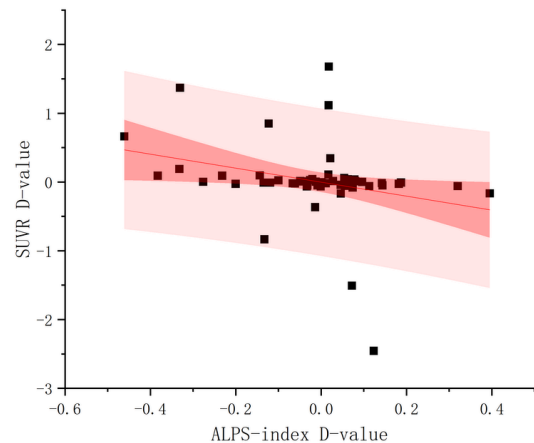
(D) GMV D-value ~WMV D-value



(E) GMVF D-value ~MMSE Scores D-value (GMA)



(F) 18 F-AV45 SUVR D-value ~ALPS-index D-value(GMA)

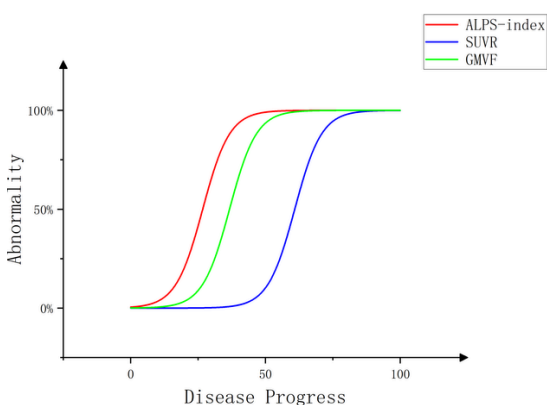


Sequential changes in SUVR of 18 F-AV45 PET images, GMVF, and ALPS-index in relation to cognitive dysfunction

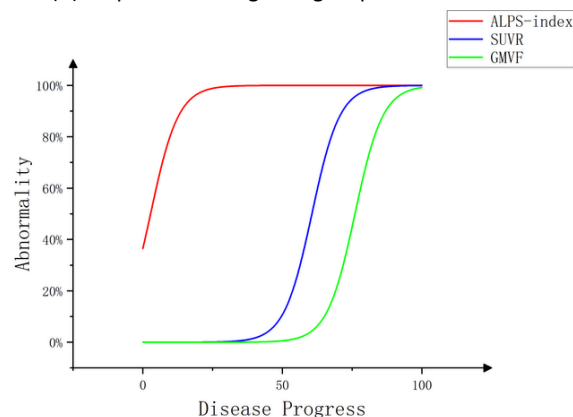
Using PACC scores as a proxy for disease progression (with larger values on the X-axis indicating more severe disease progression), a sigmoid four-parameter curve fitting model revealed that the fitting curves for ALPS-index, GMVF, and regional SUVR gradually rise with disease progression and then reached a plateau (Figure 5A). Quantitative analysis of all data showed that the PACC scores at the inflection point of the Sigmoid curve were highest for the SUVR curve (60.88), followed by the GMVF curve (36.64), and the ALPS-index curve (26.71), suggesting that the acceleration inflection point of the ALPS-index may precede changes in A β PET deposition and GMVF. Nonlinear fitting models for the MCI-AD (Figure 5B), A β + PET group (Figure 5C), and A β - PET group (Figure 5D) showed that the PACC scores at the inflection point of the Sigmoid curve were highest for the SUVR curve, indicating that the acceleration inflection point of the ALPS-index may precede A β PET deposition. Nonlinear fitting models for the MCI (Figure 5E), AD (Figure 5F), CN (Figure 5G), APOE4+ group (Figure 5H), and APOE4- group (Figure 5I) showed that the PACC scores at the inflection point of the Sigmoid curve were highest for the ALPS-index curve, suggesting that the acceleration inflection point of the ALPS-index may follow A β deposition.

Figure 5

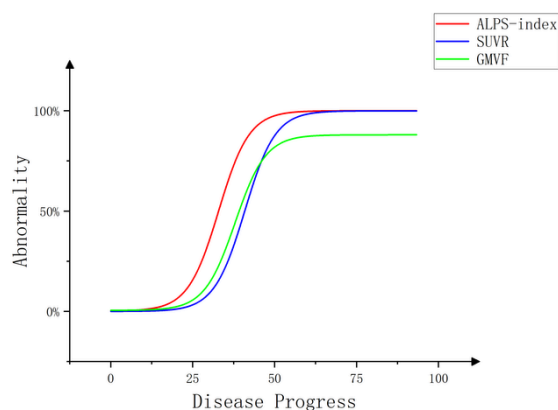
(A) Sequential changes of all data



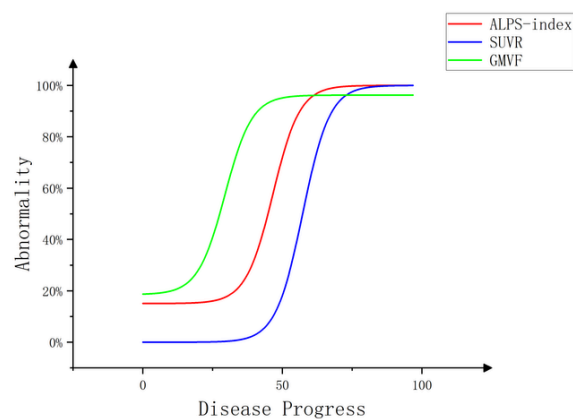
(B) Sequential changes in group MCI-AD



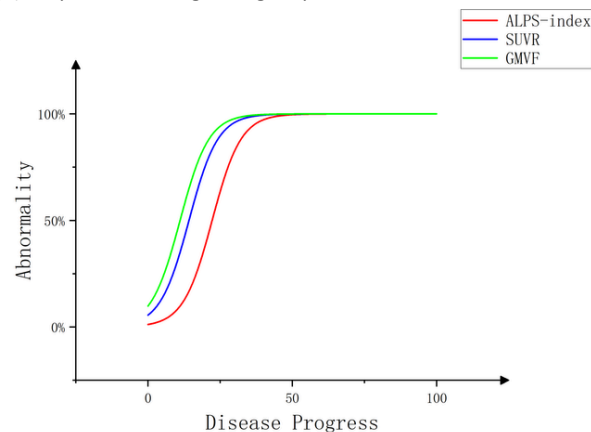
(C) Sequential changes in group A β +PET



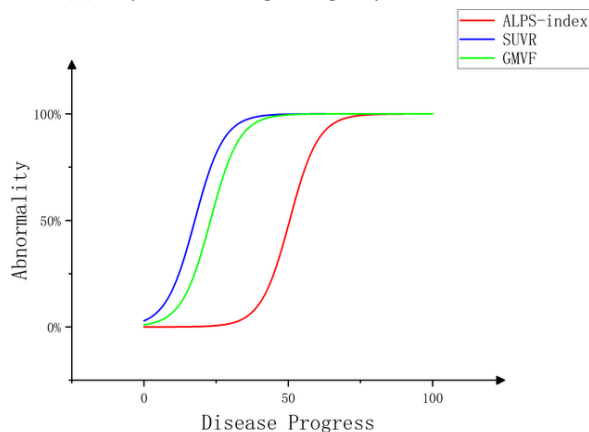
(D) Sequential changes in group A β -PET



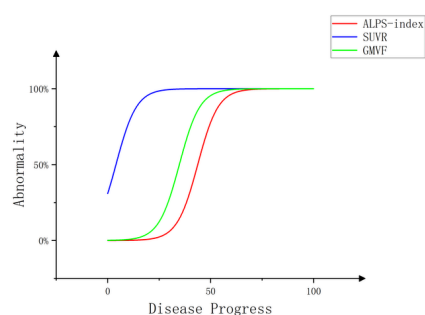
(E) Sequential changes in group MCI



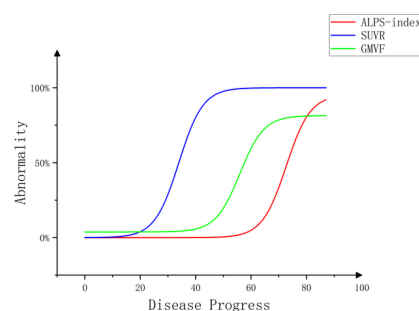
(F) Sequential changes in group AD



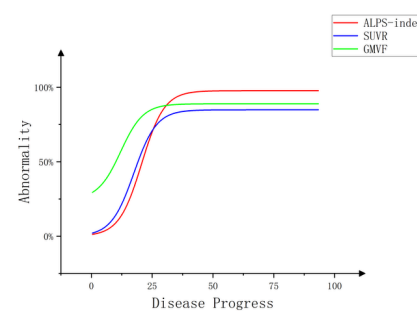
(G) Sequential changes in group CN



(H) Sequential changes in group APOE4+



(I) Sequential changes in group APOE4-



ALPS-index as a significant mediator between deposition of β -amyloid and cognitive dysfunction

In the mediation analysis of regional $A\beta$ deposition, after controlling for multiple covariates, the ALPS-index demonstrated significant full mediation effects between regional SUVR and CDR-SB scores (indirect effect(IE) = 0.56, 95% [CI] = 0.19 ~ 1.13; direct effect(DE) = 0.26, 95% [CI] = -1.04 ~ 1.56; total effect(TE) = 0.81, 95% [CI] = -0.45 ~ 2.08; Pm=68.27%), MMSE scores (IE = -0.75, 95% [CI] = -1.60 ~ -0.27; DE = -0.22, 95% [CI] = -1.87 ~ 1.43; TE = -0.96, 95% [CI] = -2.57 ~ 0.65; Pm=77.28%), and PACC scores (IE = -2.69, 95% [CI] = -5.76 ~ -0.76; DE = -1.67, 95% [CI] = -8.42 ~ 5.08; TE = -4.36, 95% [CI] = -10.92 ~ 2.21; Pm=61.61%). The ALPS-index in the CI group showed significant full mediation effects between SUVR and MMSE scores, and PACC scores. The ALPS-index in the APOE4-group showed significant full mediation effects between SUVR and CDR-SB scores, MMSE scores, and PACC scores. The ALPS-index in the $A\beta$ +PET group showed significant full mediation effects between SUVR and CDR-SB scores, MMSE scores, and PACC scores. The mediation analysis percentage (Pm) of the ALPS-index between regional $A\beta$ deposition and clinical cognitive scores is shown in Table 3.

TABLE 3. Pm (%) of ALPS index between cognitive score and GMVF

M	X	Y	Total (N=170)	CI (N=114)	$A\beta$ +PET (N=90)	APOE4- (N=94)
ALPS-index	SUVR	CDR-SB	68.27		99.17	68.95
	SUVR	MMSE	77.28	81.09	80.91	97.32
	SUVR	PACC	61.61	55.57	69.4	93.21
	SUVR	GMVF				

Table 3 Notes: Raw data were presented as mean (\pm standard deviation [SD]) or number (percentage, %) in tables unless otherwise noted. There was no mediation relationship between ALPS-index, SUVR, and GMVF

Abbreviations: ALPS, diffusion tensor image analysis along the perivascular space; $A\beta$, amyloid beta; $A\beta$ +PET, $A\beta$ PET positive; APOE4, apolipoprotein E4; CDR-SB, Clinical Dementia Rating Sum of Boxes; CI, cognitive impairment; GMVF, gray matter volume fraction; MMSE, Mini-Mental State Examination; PACC, Preclinical Alzheimer's Cognitive Composite; SUVR, standardized uptake value ratio.

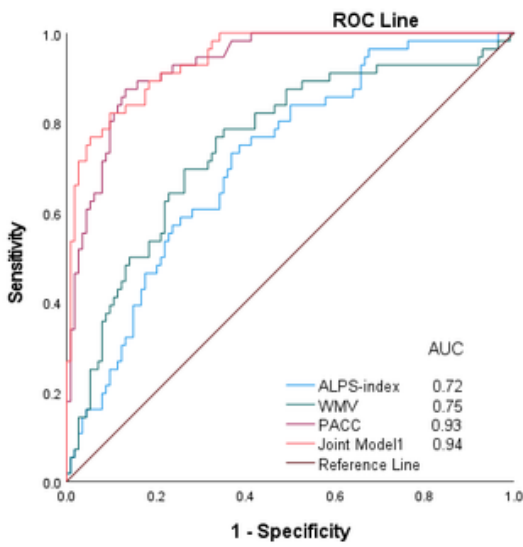
ALPS index predicts clinical progression in AD as well as $A\beta$ -positive transition

The ALPS-index, PACC scores, and WMV exhibited significant differences between the CI and CN groups, predicting patient disease progression through a binary Logistic regression model ($p < 0.001$), respectively. Joint Model 1 (Figure 6A) fit well ($X^2 = 14.84$, $P = 0.06 > 0.05$), better predicting the probability of normal patients developing cognitive impairment (AUC=0.94, $p < 0.001$) and outperforming individual predictive factors in forecasting AD clinical progression (AUC=0.96, $p < 0.001$, Figure 6C). MOCA scores, PACC scores, and MMSE scores demonstrated significant differences between the $A\beta$ -PET and $A\beta$ +PET groups. Joint Model 2 (Figure 6E), which was established in conjunction with the ALPS-index ($X^2 = 2.79$, $P = 0.947 > 0.05$), was able to better predict $A\beta$ -positive conversion (AUC=0.69, $p = 0.006$).

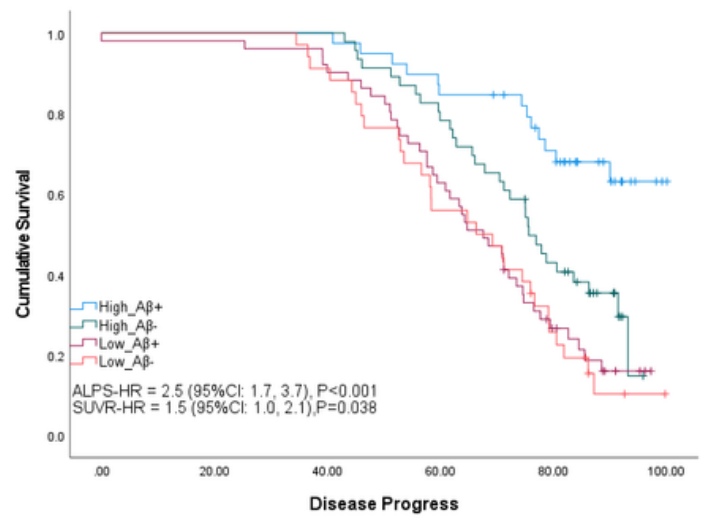
A lower ALPS-index represented a more severe degree of glymphatic system impairment, increasing the risk of patients developing cognitive impairment (hazard ratio, HR = 2.5(95%CI: 1.7, 3.7), $p < 0.001$). $A\beta$ -PET indicated the absence of significant $A\beta$ deposition in the patient's brain, which also increased the risk of cognitive impairment (HR = 1.5(95%CI: 1.0, 2.1), $P = 0.04$, Figure 6B). A lower ALPS-index increased the risk of normal patients and MCI patients progressing to AD (HR = 3.0(95%CI: 1.6, 5.6), $p < 0.001$), while the degree of $A\beta$ deposition did not significantly affect the clinical risk of normal patients and MCI patients converting to AD (HR = 1.4(95%CI: 0.8, 2.5), $p = 0.201$, Figure 6D). A lower ALPS-index also increased the risk of $A\beta$ -positive conversion (HR = 0.4(95%CI: 0.3, 0.7), $p < 0.001$, Figure 6F).

Figure 6

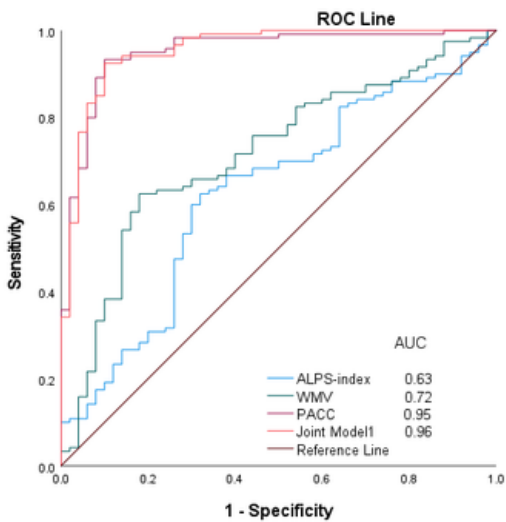
(A) Conversion to MCI/AD



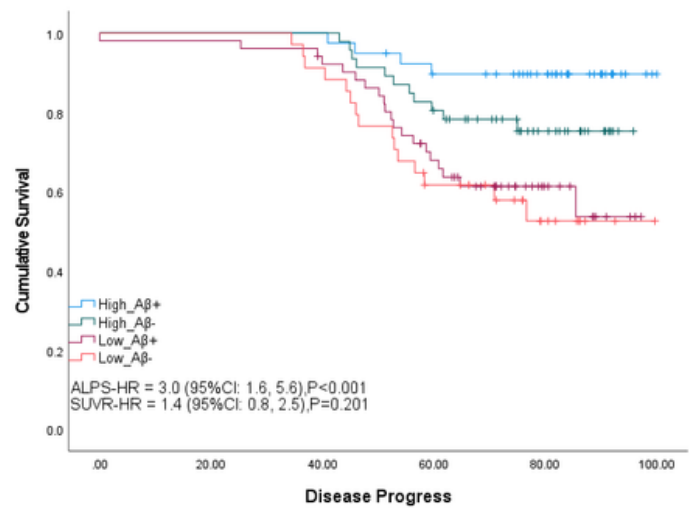
(B) Conversion to MCI/AD



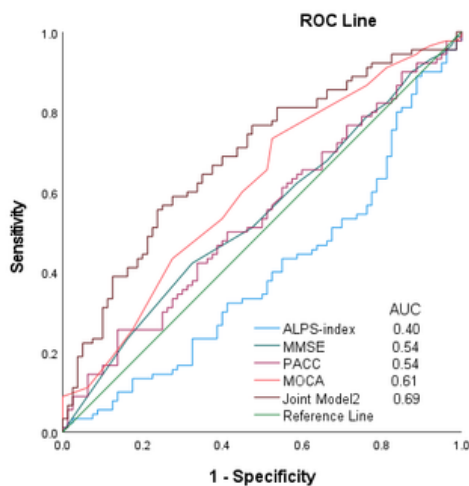
(C) Conversion from CN/MCI to AD



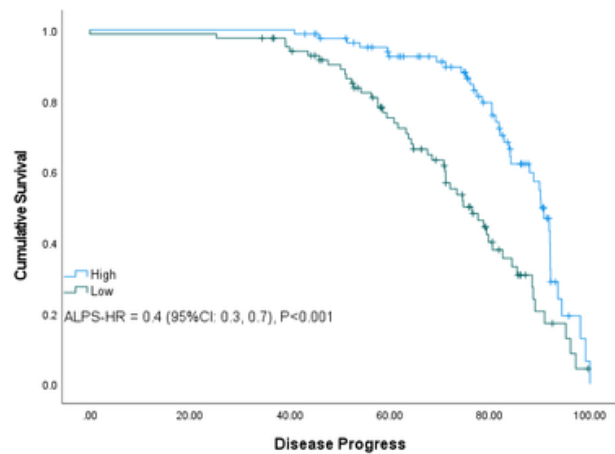
(D) Conversion from CN/MCI to AD



(E) Conversion from Aβ- to Aβ+



(F) Conversion from Aβ- to Aβ+



DISCUSSION

This study evaluated MCI and AD patients using the ALPS-index, indicative of glymphatic activity, and regional SUVR from 18 F-AV45 PET imaging, representative of A β burden. Few studies have examined the ALPS-index across various biological and pathological stages of AD. Our results fill a gap in knowledge, showing a significant reduction in the ALPS-index for MCI-AD and MCI compared to the CN control group ($p < 0.01$), suggesting the possibility of Glymphatic dysfunction at early stages of AD. AD converters exhibited more severe glymphatic system failure or damage compared to MCI patients who did not convert to AD ($p < 0.01$). There is a growing body of cross-sectional evidence associating the glymphatic system in AD A β burden and cognitive performance. Our study provides further evidence that a lower ALPS-index predicts a heavier A β burden and more severe cognitive decline ($p < 0.001$), a higher risk of A β positivity conversion (HR = 3.0(95%CI: 1.6, 5.6), $p < 0.001$), and a higher risk of AD clinical progression (HR = 2.5(95%CI: 1.7, 3.7), $p < 0.001$). The faster the decline in the ALPS-index, the quicker the A β deposition and the faster the cognitive decline ($p = 0.01$). In GMA patients, quicker gray matter atrophy is associated with faster cognitive decline ($P = 0.02$), and APOE4 carriers are more vulnerable to gray matter atrophy. The relationship between A β burden and cognitive dysfunction is fully mediated by glymphatic activity, with the temporal relationship between glymphatic system damage and A β deposition varying across different biological and pathological stages of AD.

Recent studies have demonstrated a mediating relationship between the ALPS-index, A β deposition, cognitive function, and regional gray matter volume.[25, 26] Our research offers multiple lines of evidence supporting the decisive role of glymphatic activity in A β deposition. After adjusting for several covariates, glymphatic activity may also play a substantial mediating role in AD-related cognitive dysfunction. The conversion phase of AD is relatively important in the formation of the disease. An accelerated turning point in the ALPS-index was observed earlier in the MCI-AD group than in A β abnormal deposition and brain atrophy, potentially indicating that the glymphatic system function in patients undergoing AD conversion is rapidly impaired at this stage. This stage is characterized by a rapid decline in the ALPS-index followed by rapid abnormal deposition of A β and brain atrophy. In contrast, in the CN, MCI, and AD groups, the accelerated turning points for A β load and brain atrophy were observed earlier than the ALPS-index. This implies that in normal individuals and MCI patients, under the influence of certain factors (such as age, insomnia, etc.), the glymphatic system function declines, leading to early rapid deposition of A β . However, the glymphatic system has some compensatory capacity for damage, which is reflected in the absence of a rapid decrease in the ALPS-index. It is only after the compensatory capacity of the glymphatic system is exhausted that the ALPS-index rapidly decreases, indicating a lag in the accelerated decline of the ALPS-index behind A β deposition and brain atrophy. This could be clinically interpreted as the glymphatic system in the MCI stage having a protective effect on patient cognitive function. In AD patients, the substantial and persistent A β load further impairs the glymphatic system,[27] leading to continued substantial changes in brain atrophy. Studies have shown that throughout the entire process of the occurrence of AD, the changes in glymphatic system function and the consequent abnormal deposition of A β may be divided into several accelerated stages, which mutually promote each other.

Our novel contributions encompass the longitudinal design, exploration of dynamic changes across different stages of AD, utilization of mediation models, and risk prediction. An expanding body of cross-sectional evidence linking the glymphatic system in AD with A β burden and cognitive performance. We present additional evidence that glymphatic system impairment exacerbates A β burden, elevates the risk of cognitive impairment in normal patients, progression to AD, and the risk of A β positivity conversion. We found that the ALPS-index fully mediates the relationship between A β burden and cognitive dysfunction, and cerebral glymphatic function as assessed by the ALPS-index might exert a protective effect on AD-related cognitive decline, particularly evident in the MCI stage.

Although the ALPS-index has been demonstrated[28] and studied in sleep disorders[29] and Parkinson's,[30] as well as behavioral variant frontotemporal dementia,[31] the correlation between the ALPS-index and human glymphatic system function has not yet been thoroughly validated by pathophysiological studies. Secondly, the ALPS-index assesses whole-brain glymphatic system function and does not reflect regional glymphatic system dysfunction. Hence, we should interpret the relationship between the ALPS-index and glymphatic system clearance with caution. Advancing new methods[32, 33] for measuring local glymphatic system function is our future goal. Third, care should be taken when interpreting the exact sequence of glymphatic system dysfunction and A β deposition, even though trajectory plots utilizing cognitive scores as proxies can intuitively indicate the sequence of events at various disease stages. Fourthly, we did not exclude the effects of sleep parameters, cardiovascular factors, or medication on the glymphatic system. Lastly, the predictive role of ALPS-index for amyloid, brain atrophy, and cognitive function was clearly demonstrated in our study, and although we could not accurately infer a causal relationship between them at various stages of the different biology and pathology of AD, the results of our mediation analyses suggest that they are more than just a correlation. Future studies should focus on longitudinal studies with larger sample sizes and the mechanisms through which glymphatic system function impairment directly affects brain structure.

CONCLUSION

In summary, we employed the ALPS-index to investigate the glymphatic system across various pathological and biological stages of AD, shedding light on the dynamic changes in the glymphatic system, A β deposition, and brain atrophy throughout the disease process. This research is the first in suggesting that the glymphatic system during the transition to MCI, exerts a protective effect on patients' cognitive functions. Our research underscored the predictive utility of the ALPS-index for amyloid deposition, brain atrophy, and cognitive decline in a longitudinal cohort. In patients with GMA, carriers of the APOE4 allele may face autophagy impairments that speed up gray matter atrophy, expedite cognitive decline, and promote the onset of AD. A lower ALPS-index is indicative of a higher A β burden, a faster risk of AD clinical progression, and a higher risk of conversion to A β positivity. Glymphatic activity has a complete mediating role in the association between amyloid-beta and cognitive dysfunction across different pathological and biological stages of AD. This study is the first to demonstrate that a lighter A β burden under the same glymphatic function predicts a higher risk of clinical progression of cognitive impairment, but the degree of A β burden does not significantly affect the risk of AD clinical progression. The comprehensive model proposed in this study, pertaining to the ALPS-index, exhibits robust predictive power for AD clinical progression and A β positivity conversion in the MCI stage and conversion phase of AD. Our

findings broaden the understanding of the relationship between glymphatic activity and AD pathology and clinical cognitive decline, expand the clinical application of the ALPS-index in the field of neurodegenerative disease research and treatment, and further validate the glymphatic system's impairment in the neurodegenerative pathway to AD. This provides evidence for early targeting of the glymphatic system to reduce functional impairment and subsequent amyloid deposition, neurodegeneration, and cognitive impairment during AD.

ACKNOWLEDGMENTS

The authors want to acknowledge the study participants and all the investigators involved in the Alzheimer's Disease Neuroimaging Initiative (ADNI) for their helpful contributions to data collection. Data used in preparation for this paper were obtained from the ADNI database (<http://adni.loni.usc.edu/>). As such, the investigators within the ADNI contributed to the design and implementation of ADNI and/or provided data but did not participate in analysis or writing of this report. A complete listing of ADNI investigators can be found at: http://adni.loni.usc.edu/wpcontent/uploads/how_to_apply/ADNI_Acknowledgement_List.pdf. Data collection and sharing for this project was funded by the ADNI (National Institutes of Health Grant U01 AG024904) and DOD ADNI (Department of Defense award number W81XWH-12-2-0012). ADNI is funded by the National Institute on Aging, the National Institute of Biomedical Imaging and Bioengineering, and through generous contributions from the following: AbbVie; Alzheimer's Association; Alzheimer's Drug Discovery Foundation; Araclon Biotech; BioClinica, Inc.; Biogen; Bristol-Myers Squibb Company; CereSpir, Inc.; Cogstate; Eisai Inc.; Elan Pharmaceuticals, Inc.; Eli Lilly and Company; EuroImmun; F. Hoffmann-La Roche Ltd and its affiliated company Genentech, Inc.; Fujirebio; GE Healthcare; IXICO Ltd.; Janssen Alzheimer Immunotherapy Research & Development, LLC; Johnson & Johnson Pharmaceutical Research & Development LLC; Lumosity; Lundbeck; Merck & Co., Inc.; Meso Scale Diagnostics, LLC; NeuroRx Research; Neurotrack Technologies; Novartis Pharmaceuticals Corporation; Pfizer Inc.; Piramal Imaging; Servier; Takeda Pharmaceutical Company; and Transition Therapeutics. The Canadian Institutes of Health Research is providing funds to support ADNI clinical sites in Canada. Private sector contributions are facilitated by the Foundation for the National Institutes of Health (www.fnih.org). The grantee organization is the Northern California Institute for Research and Education, and the study is coordinated by the Alzheimer's Therapeutic Research Institute at the University of Southern California. ADNI data are disseminated by the Laboratory for Neuro Imaging at the University of Southern California.

REFERENCES

- Oshio K. What Is the "Glymphatic System"? *Magn Reson Med Sci*, 2023, 22(1): 137-41.
- Hunter T R, Santos L E, Tovar-Moll F, et al. Alzheimer's disease biomarkers and their current use in clinical research and practice. *Mol Psychiatry*, 2024.
- Zhang Y, Jiang J, Ling R, et al. Early Diagnosis and Biomarkers of Alzheimer's Disease Based on Spatio-temporal Graph Convolution Network. *5th Annual International Conference of the IEEE Engineering in Medicine & Biology Society (EMBC) 2023*.
- Iliff J J, Wang M, Liao Y, et al. A paravascular pathway facilitates CSF flow through the brain parenchyma and the clearance of interstitial solutes, including amyloid beta. *Sci Transl Med*, 2012, 4(147): 147ra11.
- Iliff J J, Chen M J, Plog B A, et al. Impairment of glymphatic pathway function promotes tau pathology after traumatic brain injury. *J Neurosci*, 2014, 34(49): 16180-93.
- [6] Ota M, Sato N, Nakaya M, et al. Relationships Between the Deposition of Amyloid- β and Tau Protein and Glymphatic System Activity in Alzheimer's Disease: Diffusion Tensor Image Study. *J Alzheimers Dis*, 2022, 90(1): 295-303.
- Rye I, Vik A, Kocinski M, et al. Predicting conversion to Alzheimer's disease in individuals with Mild Cognitive Impairment using clinically transferable features. *Scientific Reports*, 2022, 12(1): 15566.
- Jack C R, Jr., Wiste H J, Vemuri P, et al. Brain beta-amyloid measures and magnetic resonance imaging atrophy both predict time-to-progression from mild cognitive impairment to Alzheimer's disease. *Brain*, 2010, 133(11): 3336-48.
- Gallego-Rudolf J, Wiesman A I, Pichet Binette A, et al. Synergistic association of A β and tau pathology with cortical neurophysiology and cognitive decline in asymptomatic older adults. *Nature Neuroscience*, 2024, 27(11): 2130-7.
- Taoka T, Ito R, Nakamichi R, et al. Reproducibility of diffusion tensor image analysis along the perivascular space (DTI-ALPS) for evaluating interstitial fluid diffusivity and glymphatic function: CHanges in Alps index on Multiple conditiON acqLisition eXperiment (CHAMONIX) study. *Jpn J Radiol*, 2022, 40(2): 147-58.
- Jack C R, Jr., Knopman D S, Jagust W J, et al. Tracking pathophysiological processes in Alzheimer's disease: an updated hypothetical model of dynamic biomarkers. *Lancet Neurol*, 2013, 12(2): 207-16.
- Nedergaard M, Goldman S A. Glymphatic failure as a final common pathway to dementia. *Science*, 2020, 370(6512): 50-6.
- Donohue M C, Sperling R A, Salmon D P, et al. The preclinical Alzheimer cognitive composite: measuring amyloid-related decline. *JAMA Neurol*, 2014, 71(8): 961-70.
- Mormino E C, Papp K V, Rentz D M, et al. Early and late change on the preclinical Alzheimer's cognitive composite in clinically normal older individuals with elevated amyloid beta. *Alzheimers Dement*, 2017, 13(9): 1004-12.
- Kanekiyo T, Xu H, Bu G. ApoE and Abeta in Alzheimer's disease: accidental encounters or partners?. *Neuron*, 2014, 81(4): 740-54.
- Corder E H, Saunders A M, Strittmatter W J, et al. Gene dose of apolipoprotein E type 4 allele and the risk of Alzheimer's disease in late onset families. *Science*, 1993, 261(5123): 921-3.
- Martinez-Morillo E, Hansson O, Atagi Y, et al. Total apolipoprotein E levels and specific isoform composition in cerebrospinal fluid and plasma from Alzheimer's disease patients and controls. *Acta Neuropathol*, 2014, 127(5): 633-43.
- Asiamah E A, Feng B, Guo R, et al. The Contributions of the Endolysosomal Compartment and Autophagy to APOE ϵ 4 Allele-Mediated Increase in Alzheimer's Disease Risk. *Journal of Alzheimer's Disease*, 2024, 97: 1007-31.
- Palmqvist S, Mattsson N, Hansson O, et al. Cerebrospinal fluid analysis detects cerebral amyloid-beta accumulation earlier than positron emission tomography. *Brain*, 2016, 139(Pt 4): 1226-36.
- Bateman R J, Xiong C, Benzinger T L, et al. Clinical and biomarker changes in dominantly inherited Alzheimer's disease. *N Engl J Med*, 2012, 367(9): 795-804.
- Cwiek-Ludwicka K, Jedrzejczak R. [Codex foodstuffs committee FAO/WHO on methods of analysis and sampling]. *Rocz Panstw Zakl Hig*, 1994, 45(3): 207-14.

22. Schindler S E, Gray J D, Gordon B A, et al. Cerebrospinal fluid biomarkers measured by Elecsys assays compared to amyloid imaging. *Alzheimers Dement*, 2018, 14(11): 1460-9.
23. MacKinnon D P, Valente M J, Gonzalez O. The Correspondence Between Causal and Traditional Mediation Analysis: the Link Is the Mediator by Treatment Interaction. *Prev Sci*, 2020, 21(2): 147-57.
24. Hayes A F. Introduction to mediation, moderation, and conditional process analysis: A regression-based approach. New York, NY, US; Guilford Press, 2013.
25. Hsu J L, Wei Y C, Toh C H, et al. Magnetic Resonance Images Implicate That Glymphatic Alterations Mediate Cognitive Dysfunction in Alzheimer Disease. *Annals of Neurology*, 2022, 93(1): 164-74.
26. Huang S Y, Zhang Y R, Guo Y, et al. Glymphatic system dysfunction predicts amyloid deposition, neurodegeneration, and clinical progression in Alzheimer's disease. *Alzheimers Dement*, 2024, 20(5): 3251-69.
27. Peng W, Achariyar T M, Li B, et al. Suppression of glymphatic fluid transport in a mouse model of Alzheimer's disease. *Neurobiol Dis*, 2016, 93: 215-25.
28. Zhang W, Zhou Y, Wang J, et al. Glymphatic clearance function in patients with cerebral small vessel disease. *Neuroimage*, 2021, 238: 118257.
29. Xiong Z, Bai M, Wang Z, et al. Resting-state fMRI network efficiency as a mediator in the relationship between the glymphatic system and cognitive function in obstructive sleep apnea hypopnea syndrome: Insights from a DTI-ALPS investigation. *Sleep Med*, 2024, 119: 250-7.
30. Si X, Guo T, Wang Z, et al. Neuroimaging evidence of glymphatic system dysfunction in possible REM sleep behavior disorder and Parkinson's disease. *NPJ Parkinsons Dis*, 2022, 8(1): 54.
31. Jiang D, Liu L, Kong Y, et al. Regional Glymphatic Abnormality in Behavioral Variant Frontotemporal Dementia. *Ann Neurol*, 2023, 94(3): 442-56.
32. Naganawa S, Taoka T. The Glymphatic System: A Review of the Challenges in Visualizing its Structure and Function with MR Imaging. *Magn Reson Med Sci*, 2022, 21(1): 182-94.
33. Watts R, Steinklein J M, Waldman L, et al. Measuring Glymphatic Flow in Man Using Quantitative Contrast-Enhanced MRI. *AJNR Am J Neuroradiol*, 2019, 40(4): 648-51.

Figure Legends:

Figure 1 : (A) Overview of the study. (B) The original T1-weighted images and PET imaging registration process. (C) Segmentation of gray matter, white matter, and cerebrospinal fluid using the subject's T1-weighted images. (D) The calculation process of the regional SUVR for 18 F-AV45 PET images, ROIs include the following areas: the precentral gyrus, olfactory cortex, anterior and posterior cingulate cortices, precuneus, hippocampus, parahippocampal gyrus, amygdala, cuneus, caudate nucleus, and thalamus. (E) The process of calculating the ALPS-index through original diffusion-weighted imaging (DTI) images. (F) A schematic diagram showing the relationship between the direction of PVS (red cylinders) and the orientation of nerve fibers in the left hemisphere of the brain, with X(F-H) indicating the projection fiber direction along the foot-to-head axis. ALPS, diffusion tensor image analysis along the PVS. AP-, bvec and bval, text files for the different content; FA-RGB, fractional anisotropy red-green-blue three-color code; MNI, Montreal Neurological Institute; SUVR, standardized uptake value ratio.

Figure 2 : The bar scatter plots were used to visualize the differential data between groups. (A) There are significant differences in WMV, CSFV, ALPS-index, CDR-SB scores, FAQ scores, MMSE scores, PACC scores, and MOCA scores between the CI and CN groups. (B) For the AD, MCI-AD, MCI, and CN groups, there are significant differences in WMV and CSFV, ALPS-index, as well as FAQ scores, MOCA scores, MMSE scores, CDR-SB scores, and PACC scores among the four groups. (C) There are significant differences in regional SUVR of 18 F-AV45 PET images, MOCA scores, pTau concentration, A β concentration, and tTau concentration between the CSF A β + and CSF A β - groups. (D) There are significant differences in MOCA scores, MMSE scores, and PACC scores between the A β +PET and A β -PET groups. Moreover, there are significant differences in ICV, GMV, CSFV, and MOCA scores between the APOE4+ and APOE4- groups. ALPS, diffusion tensor image analysis along the perivascular space; AD, Alzheimer's disease; ABETA, amyloid beta (A β); APOE4, apolipoprotein E4; CI, cognitive impairment; CN, Cognitively normal; CDR-SB, Clinical Dementia Rating Sum of Boxes; CSFV, cerebrospinal fluid volume; FAQ, Functional Activities Questionnaire; MCI, Mild cognitive impairment; CSF A β +, cerebrospinal fluid A β positive; CSF A β -, Cerebrospinal fluid A β negative; MCI-AD, MCI patients who converted to AD; MOCA, Montreal Cognitive Assessment; MMSE, Mini-Mental State Examination; PTAU, phosphorylated tau protein; PACC, Preclinical Alzheimer's Cognitive Composite; TTAU, total tau protein; SUVR, standardized uptake value ratio.

Figure 3 : After controlling for age, gender, years of education, and APOE4 genotype, the DTI-ALPS index was correlated with the regional standardized uptake value ratio (SUVR) from 18 F-AV45 PET imaging, MMSE scores, and PACC scores. In the CI group, the DTI-ALPS index was correlated with the average SUVR of 18 F-AV45 PET images and the regional SUVR was correlated with GMV. In the MCI group, the ALPS index was correlated with the regional SUVR of 18 F-AV45 PET imaging. In the AD group, the regional SUVR of 18 F-AV45 PET imaging was correlated with ICV. In the CN group, the ALPS index was correlated with ICV, regional SUVR of 18 F-AV45 PET imaging, and CSFV. (A) The ALPS index was significantly negatively correlated with regional SUVR ($R^2 = 0.06$, $p = 0.001$). (B) The ALPS index showed significantly positive correlation with MMSE scores ($R^2 = 0.07$, $p < 0.001$). (C) The ALPS index showed significantly positive correlation with PACC scores ($R^2 = 0.07$, $p < 0.001$). (D) In the CI group, the ALPS index was significantly negatively correlated with regional SUVR ($R^2 = 0.08$, $p < 0.01$). (E) In the CI group, the regional SUVR is significantly negatively correlated with GMV ($R^2 = 0.04$, $p = 0.02$). (F) In the MCI group, the ALPS index was significantly negatively correlated with regional SUVR ($R^2 = 0.14$, $p = 0.006$). (G) In the AD group, the regional SUVR was significantly negatively correlated with ICV ($R^2 = 0.06$, $p = 0.04$). (H) In the CN group, the ALPS index was significantly negatively correlated with ICV ($R^2 = 0.18$, $p = 0.03$). (I) In the CN group, the regional SUVR was significantly positively correlated with CSFV ($R^2 = 0.09$, $p = 0.04$). ALPS, diffusion tensor image analysis along the perivascular space; CI, cognitive impairment; CN,

cognitively normal; CSFV, cerebrospinal fluid volume; GMV, gray matter volume; ICV, intracranial volume; MCI, Mild cognitive impairment; MMSE, Mini-Mental State Examination; SUVR, standardized uptake value ratio.

Figure 4 : Longitudinal analysis revealed that the ALPS-index is associated with SUVR and ICV, while WMV is associated with GMV and CSFV. For GMA patients, the ALPS-index was related to SUVR and GMVF. After controlling for gender, age, APOE4 genotype, and years of education, the following significant correlations were found:(A) The D-value of the ALPS-index is significantly negatively correlated with the D-value of SUVR ($R^2=0.07$, $p=0.01$). (B) The D-value of the SUVR was significantly negatively correlated with the D-value of ICV ($R^2=0.01$, $p=0.04$). (C) The D-value of WMV was significantly negatively correlated with the D-value of GMV ($R^2=0.50$, $p<0.01$). (D) The D-value of WMV was significantly negatively correlated with the D-value of CSFV ($R^2=0.16$, $p<0.01$). (E) For GMA patients, the D-value of GMVF was significantly positively correlated with the D-value of MMSE scores ($R^2=0.03$, $p=0.02$). (F) For GMA patients, the D-value of the ALPS-index was significantly negatively correlated with the D-value of SUVR ($R^2=0.08$, $p=0.03$). ALPS, diffusion tensor image analysis along the perivascular space; D-value, difference value; GMV, gray matter volume; ICV, intracranial volume; MMSE, Mini- Mental State Examination; SUVR, standardized uptake value ratio.

Figure 5 : A joint fit analysis of the regional SUVR from 18 F-AV45 PET imaging, the ALPS-index, and GMVF was conducted to analyze their sequential changes in relation to cognitive dysfunction. The regional SUVR, ALPS-index, and GMVF were normalized to a 0 to 100% scale, with 0% being the minimum and 100% the maximum for SUVR, and 0% the maximum and 100% the minimum for ALPS and GMVF. This standardization process made the abnormal values of regional SUVR, GMVF, and ALPS-index higher, with higher values on the Y-axis indicating a more severe disease state. The X-axis coordinates were derived from $(1 - \text{normalized PACC scores}) * 100$, with higher values on the X-axis representing a more advanced disease progression. (A) The inflection point of the SUVR curve (60.88) was greater than that of the GMVF curve (36.64) and the ALPS-index curve (26.71). (B) In the MCI-AD group, the inflection point of the GMVF curve (76.03) was greater than that of the SUVR curve (60.60) and the ALPS-index curve (2.77). (C) In the A β +PET group, the inflection point of the SUVR curve (32.70) was greater than that of the GMVF curve (30.34) and the ALPS-index curve (26.34). (D) In the A β -PET group, the inflection point of the SUVR curve (57.28) was greater than that of the ALPS-index curve (46.57) and the GMVF curve (29.40). (E) In the MCI group, the inflection point of the ALPS-index curve (22.22) was greater than that of the SUVR curve (14.20) and the GMVF curve (11.11). (F) In the AD group, the inflection point of the ALPS-index curve (50.47) was greater than that of the GMVF curve (23.02) and the SUVR curve (17.61). (G) In the CN group, the inflection point of the ALPS-index curve (43.72) was greater than that of the GMVF curve (34.79) and the SUVR curve (4.02). (H) In the APOE4+ group, the inflection point of the ALPS-index curve (72.70) was greater than that of the GMVF curve (55.96) and the SUVR curve (33.92). (I) In the APOE4- group, the inflection point of the ALPS-index curve (16.55) was greater than that of the SUVR curve (13.98) and the GMVF (9.62), furthermore, the reduced ALPS-index precedes A β in reaching the threshold. ALPS, diffusion tensor image analysis along the perivascular space; AD, Alzheimer's disease; A β , amyloid beta; APOE4, apolipoprotein E4; CI, cognitive impairment; CN, Cognitively normal; GMVF, gray matter volume fraction; CSF A β +, cerebrospinal fluid A β positive; CSF A β -, Cerebrospinal fluid A β negative; MCI, Mild cognitive impairment; MCI-AD, MCI patients who converted to AD; SUVR, standardized uptake value ratio.

Figure 6 : Utilizing ROC curves to compare the predictive performance of the ALPS-index integrated model and individual predictive factors, PACC scores were used as an indicator of disease progression time (higher values indicating more severe disease) to plot Kaplan-Meier curves, revealing that the ALPS-index and SUVR are associated with the risk of clinical progression of AD and A β positivity conversion. (A) Comparison of the performance between Joint Model 1 (ALPS-index + PACC scores + WMV) and individual predictive factors, Joint Model 1 ($AUC=0.94 > 0.93 > 0.75 > 0.72$, $p<0.001$) has superior ability in predicting cognitive impairment in patients compared to individual predictive factors. (B) Kaplan-Meier curves for the occurrence of cognitive impairment in patients. (C) Comparison of the performance between Joint Model 1 (ALPS-index + PACC scores + WMV) and individual predictive factors, Joint Model 1 ($AUC=0.96 > 0.95 > 0.72 > 0.63$, $p<0.001$) has superior ability in predicting AD clinical progression compared to individual predictive factors. (D) Kaplan-Meier curves for the progression from CN patients to AD and from MCI patients to AD. (E) Comparison of the performance between Joint Model 2 (ALPS-index + PACC scores + MMSE scores + MOCA scores) and individual predictive factors, Joint Model 2 ($AUC=0.69 > 0.61 > 0.54 > 0.54 > 0.40$, $p<0.001$) has superior ability in predicting A β positivity conversion in patients compared to individual predictive factors. (F) Kaplan-Meier curves for A β positivity conversion in patients. ALPS, diffusion tensor image analysis along the perivascular space; AD, Alzheimer's disease; APOE, apolipoprotein E; CN, cognitively normal; CI, confidence interval; MCI, mild cognitive impairment; MOCA, Montreal Cognitive Assessment; HR, hazard ratio; PACC, Preclinical Alzheimer's Cognitive Composite; WMV, white matter volume; SUVR, standardized uptake value ratio.

How to Cite: Li S, Zhang J, Wang W, Zhou S, Wang H, Sun M et al. From glymphatic system dysfunction to alzheimer's disease: Mapping the path of neurodegeneration. *Radiol Med*. 2025 Dec;19(3): 33-50